



Heat transfer enhancement with liquid–gas flow in microchannels and the effect of thermal boundary layer



Farzad Houshmand, Yoav Peles*

Department of Mechanical, Aerospace, and Nuclear Engineering, Rensselaer Polytechnic Institute, 110, 8th street, Troy, New York 12180, USA

ARTICLE INFO

Article history:

Received 5 September 2013

Received in revised form 15 November 2013

Accepted 15 November 2013

Available online 12 December 2013

Keywords:

Bubbles

Microchannel

Convective heat transfer

Two-phase flow

Heat transfer enhancement

Thermal boundary layer

ABSTRACT

Heat transfer coefficient of air–water two-phase flow in a microchannel was experimentally studied and the effect of the thermal boundary layer on the heat transfer process was elucidated. Air stream was injected into liquid water flow in a 210 μm deep and 1.5 mm wide horizontal microchannel, and the heat transfer coefficients due to the presence of bubbles were measured through an array of heaters and resistance temperature detectors (RTDs) inside the channel. Using different configurations of heated areas in the channel, the mixing effect of the bubbles and the interaction with the thermal boundary layer were studied for a range of liquid and gas flow rates. With two-phase flow, enhancement of up to 100% in the heat transfer coefficient was observed compared to single-phase flow. The enhancement was observed to be more significant for thermally developing flow with thicker thermal boundary layers.

© 2013 Elsevier Ltd. All rights reserved.

1. Introduction

Convective heat transfer in microchannels, especially for electronic cooling applications, has been a topic of much interest (e.g., [1]) ever since the early work of Tuckerman and Pease [2]. Over the years, various methods were developed to enhance heat transfer at the microscale, such as impinging jets [3], shear-driven flow [4], segmented flow [5,6], and extended surfaces [7–11].

Injection of gas bubbles into liquid flow (i.e., non-boiling gas–liquid two-phase flow) is a technique that can be triggered upon demand locally or at the system level, and similar to other active techniques, holds key advantages compared to passive approaches. In addition, knowledge about the processes controlling such flow can assist revealing the interaction of vapor bubbles with liquid flow during flow boiling. Although gas–liquid two-phase flow heat transfer is common (especially in chemical engineering applications), studies at the microscale are scarce (e.g., [12,13]). In a previous study by Houshmand and Peles [14], the effect of injected immiscible air bubbles on heat transfer and flow field in a microchannel was experimentally studied. A notable difference in the heat transfer enhancement was observed relative to other gas–liquid studies, such as the study of Betz and Attinger [5]. Comparison of the micro devices and the experimental conditions suggested that the thermal boundary layer thickness in the chan-

nel was a key difference between the experiments, requiring further investigation. Independently, the effect of developing flow on heat transfer in microchannels has been discussed in previous studies [15,16], and other studies, such as [17–19], have leveraged this concept to design more efficient micro devices.

In this study, a new set of micro devices was designed and fabricated to study the interaction of injected bubbles with the thermal boundary layer; its effect on the heat transfer process was carefully examined. Disruption of the thermal boundary layer brings colder liquid closer to the heated surface and, as a result, enhances heat transfer. It is believed that characterization of the thermal boundary layer in the test section and careful analysis of the associated conjugate effects help assess and compare the heat transfer measurements in different studies.

2. Experimental setup and method

2.1. Microdevice

To study the interaction of the injected bubbles and the thermal boundary layer, a microchannel with multiple heaters and wall temperature sensors was designed and fabricated. With multiple-heater configuration, the length of the heated area was varied, and consequently, the thickness of the thermal boundary layer was controlled.

A schematic of the microdevice is shown in Fig. 1. Distilled water flowed into a 210 μm deep, 1.5 mm wide, and 22 mm long microchannel; air bubbles were injected into the microchannel

* Corresponding author. Tel.: +1 (518) 276 2886; fax: +1 (518) 276 2623.

E-mail addresses: farzad.houshmand@gmail.com (F. Houshmand), pelesy@rpi.edu (Y. Peles).

Nomenclature

a	half-depth of the channel (m)	Re	Reynolds number (–)
A_c	cross sectional area (m ²)	t_{eq}	equivalent thickness (m)
A_H	heater area (m ²)	T_0	inlet temperature (C)
c_p	specific heat (J/kg·K)	T_{RTD}	RTD temperature (C)
D_h	hydraulic diameter (m)	T_w	wall temperature (C)
E	enhancement factor (–)	U	mid-plane (maximum) velocity (m/s)
h	heat transfer coefficient (W/m·K)	\bar{u}	average velocity (m/s)
H	channel depth (m)	W	channel width (m)
j_i	superficial velocity of fluid i (m/s)	x	axial length (m)
k_{eq}	equivalent thermal conductivity (W/m·K)	y	vertical distance from wall (m)
k_l	liquid thermal conductivity (W/m·K)	α	thermal diffusivity (m ² /s)
Nu	Nusselt number (–)	Γ_i	volumetric flow rate of fluid i (m ³ /s)
q''	heat flux (W/m ²)	δ_τ	thermal boundary layer thickness (m)
Q_{loss}	power loss (W)	μ_i	viscosity of fluid i (kg/m·s)
Q_{net}	net power (W)	ν	kinematic viscosity (m ² /s)
Q_{tot}	total power (W)	ρ	density (kg/m ³)

through a 250 μm diameter orifice located 13.9 mm ($x = 10.4$ mm) downstream of the inlet manifold. Titanium heaters and resistance temperature detectors (RTDs) were embedded in the channel to dissipate heat to the flow and directly measure the wall temperature, respectively. Heater #1 (located 3.5 mm downstream of the inlet manifold) served as a pre-heater; it allowed the thermal boundary layer, upstream of the bubble injection orifice, to grow. The flow temperature upstream of the bubbles was also controlled through the power delivered to Heater #1, and the corresponding wall temperature was measured by RTD #1. Heater #4 was the main test section of the channel, where the other four RTDs were located.

The micro device consisted of two processed Pyrex substrates and a patterned double-side adhesive-coated vinyl layer that bonded them together (Fig. 2). Four 120 nm thick and 1 mm wide heaters, and five 70 nm thick RTDs (Table 1) were formed on the bottom Pyrex substrate through a sequence of deposition and wet etching steps in a cleanroom environment. Initially, the four heaters were formed on the substrate, and after depositing a 1 μm thick layer of silicon dioxide—to electrically insulate the RTDs from the heaters beneath—the five RTDs were planted on top of the heaters. A 250 nm thick layer of silicon dioxide as well as a 150 nm thick layer of silicon nitride were also deposited on the top to electrically insulate the RTDs from the water. Subsequently, insulating layers on top of the contact pads were etched away to provide contact between the device and the electrical loop through spring loaded probe pins. Finally, the inlet and outlet

manifolds ($D = 1$ mm), as well as the bubble injection orifice, were drilled through the bottom substrate. To form the heaters and the RTDs, a layer of titanium followed by a layer of aluminum were sputtered on the surface. The electric vias and pads were covered with patterned photoresist and the remaining aluminum was removed. After rinsing the photoresist, the heater area and the aluminum patches were covered and the rest of the titanium was etched away. As a result, the exposed titanium area formed the heaters and RTDs and the low-resistance layer of aluminum composed the electric pads and vias. The final cross-section of the bottom Pyrex substrate is shown in Fig. 3 for the heaters (left) and the RTDs (right).

The vinyl layer was patterned with a laser-cutting machine (Hurricane 80 W) to form the microchannel and the access holes for the probe pins over the contact pads. Similar holes were also drilled in the Pyrex substrate that formed the top wall of the microchannel. The transparent Pyrex layer on the top enables flow visualization during experiments. After aligning and bonding the three substrates, individual devices were cut out using a die-saw.

2.2. Device packaging

To connect the micro device to the fluid lines and the measurement apparatus, a two-piece packaging system was designed and built (Fig. 4). The micro device sits in the groove on the Delrin® block, which connects the inlet and outlet ports of the microchannel to the supply connector and the drain pipe; it also connects the bubble injection orifice to the syringe pump. A set of miniature O-rings were used in the grooves beneath the fluidic ports to seal the connections between the device and the package. A set of similar O-rings was placed beneath the device to provide a uniform and elastic support and to provide an air gap between the device and the package to minimize heat loss.

The cover plate (Fig. 4(b) and (c)) consisted of a printed circuit board (PCB) substrate with soldered gold-plated probe pins and a male insulation-displacement connector (IDC) supported by a reinforcing Delrin® piece. The cover plate provided the electrical connections between the contact pads on the micro device, power supplies, and data acquisition system (DAQ) through the IDC ribbon cables. It also supported the micro device and compressed the O-rings to ensure proper sealing of the device. A window was machined in the center of the cover plate to enable flow visualization during the experiments. It should be noted that the overall

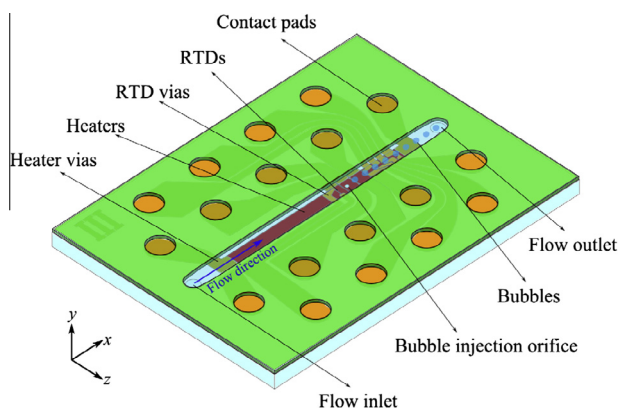


Fig. 1. A schematic of the microdevice (top Pyrex layer removed).

Download English Version:

<https://daneshyari.com/en/article/657636>

Download Persian Version:

<https://daneshyari.com/article/657636>

[Daneshyari.com](https://daneshyari.com)